

See discussions, stats, and author profiles for this publication at: <https://www.researchgate.net/publication/335735746>

Self-Assembling Peptide-Based Hydrogel: Regulation of Mechanical Stiffness and Thermal Stability and 3D Cell Culture of Fibroblasts

Article in *ACS Applied Bio Materials* · September 2019

DOI: 10.1021/acsabm.9b00424

CITATIONS

22

READS

145

8 authors, including:



Dipayan Bairagi

Indian Association for the Cultivation of Science

6 PUBLICATIONS 163 CITATIONS

[SEE PROFILE](#)



Parijat Biswas

Indian Association for the Cultivation of Science

4 PUBLICATIONS 29 CITATIONS

[SEE PROFILE](#)



Kingshuk Basu

Hebrew University of Jerusalem

21 PUBLICATIONS 445 CITATIONS

[SEE PROFILE](#)



Soumyajit Hazra

Indian Association for the Cultivation of Science

30 PUBLICATIONS 234 CITATIONS

[SEE PROFILE](#)

Some of the authors of this publication are also working on these related projects:



Nanostructure of waterborne polymer coatings [View project](#)



Design, construction and applications of peptide-based nano-materials [View project](#)

Self-Assembling Peptide-Based Hydrogel: Regulation of Mechanical Stiffness and Thermal Stability and 3D Cell Culture of Fibroblasts

Dipayan Bairagi,[†] Parijat Biswas,[†] Kingshuk Basu,[†] Soumyajit Hazra,[†] Daniel Hermida-Merino,[¶] Deepak Kumar Sinha,[†] Ian W. Hamley,[‡] and Arindam Banerjee^{*,†,¶}

[†]School of Biological Sciences, Indian Association for the Cultivation of Science, 2A & 2B Raja S. C. Mullick Road, Jadavpur, Kolkata 700032, India

[¶]ESRF – The European Synchrotron, Grenoble Cedex 38043, France

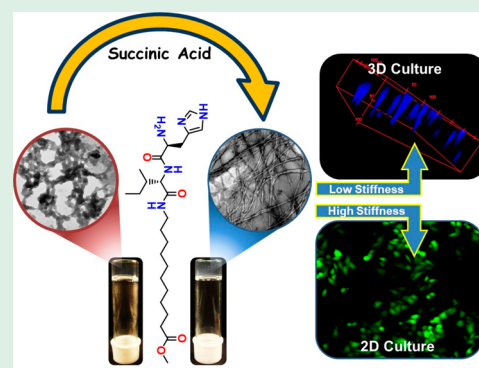
[‡]Department of Chemistry, University of Reading, Whiteknights, Reading RG6, 6AD, United Kingdom

S Supporting Information

ABSTRACT: A histidine-containing peptide-based amphiphile (P1) forms a transparent hydrogel within a pH range of 5.5 to 8.5 in phosphate buffer solution. Interestingly, thermal stability and mechanical stiffness are modulated by incorporating different types of dicarboxylic acids into the hydrogels. Inclusion of succinic acid with the molar ratio 2:1 (peptide:dicarboxylic acid) yields improved properties compared to the other tested dicarboxylic acids such as oxalic, glutaric and octanedioic acids. Transmission electron microscopic (TEM) images show the assembly of nanospheres is responsible for the hydrogel obtained from the assembly of native peptide. However, a morphological transformation takes place from nanosphere to nanofibers, when the peptide gels with succinic acid. XRD and FT-IR studies reveal interactions between peptide amphiphiles and the acids are responsible for the formation of a two-component hydrogel. Gel stiffness is enhanced considerably upon the addition of succinic acid to P1 with a 1:2 molar ratio.

The two-component gel consisting of peptide and succinic acid has been successfully used for three-dimensional cell culture using mouse fibroblast cell line (NIH-3T3). This indicates future promise for the application of such peptide-based gels as tunable biomaterials in cell culture and regenerative medicine.

KEYWORDS: peptide gels, self-assembly, tuning of gel stiffness, morphological transformation, cell culture



INTRODUCTION

Self-assembling small molecule-based soft materials have continued to create interest over the years because of their diverse applications^{1–5} and easy tunability.^{6,7} Usage of self-assembling peptides as functional materials has numerous advantages, namely, low fabrication cost, good biocompatibility, and control over functionality. Amphiphilic peptides are good candidates for self-association to form gels under suitable conditions. Current improvement of biomedical technology demands gel-like soft materials for efficient culture of stem cells,⁸ therapeutics,^{9,10} immune modulation,¹¹ in vitro diagnostics,¹² wound healing,^{13–15} creation of synthetic extracellular matrix,^{16–19} antibacterial agents,^{20–25} drug delivery,^{26–28} and many others.²⁹ For such applications, gel-forming peptides have great potential, because of their inherently biocompatible nature and low toxicity compared to conventional polymer-based materials.³⁰ Moreover, it is challenging to tune the physical properties of covalent polymers, whereas supramolecular assemblies are more flexible, and they are easily stabilized by various noncovalent interactions including H-bonding, van der Waals interactions, and π – π stacking. Design of nanofibrous gel scaffolds is one of

the key components in the field of regenerative medicine.^{31–34}

In a tissue system, the relation between the cells and the surrounding matrix plays a crucial role in proliferation, differentiation and migration of the cells for tissue repair. Hydrogels provide an excellent environment for cell growth and tissue regeneration due to their high oxygen, nutrient, and metabolite permeability. Various research groups over the globe have designed and utilized peptide-based hydrogels as cell culture scaffolds. Ulijn and co-workers reported fluorenylmethoxycarbonyl-protected peptide-based hydrogels for 3D culture of bovine chondrocytes.³⁵ Tomasini and co-workers developed a noncytotoxic pseudopeptide based hydrogel that can be used for regenerative medicine.³⁶ These peptides produce a perfect environment upon assembly which mimics the extracellular matrix as a perfect platform for the cell growth. Recently, Langhans and co-workers reported a series of β -hairpin gelator peptides for 3D cell culture.³⁷ Gazit and

Special Issue: Biomaterials Research in India

Received: May 20, 2019

Accepted: August 26, 2019

co-workers reported a peptide-based self-healing and conductive hydrogel that supported the growth of electrogenic cardiomyocytes.³⁸

In the context of cell culture, the mechanical properties of the matrix are important to realize cell adhesion and proliferation. The extracellular matrix is a dynamic system with specific mechanical properties and a rationally designed synthetic scaffold must successfully mimic the *in vivo* situation. Different types of cells demand matrices of different stiffness to grow.³⁹ Discher and co-workers have shown that it is possible to grow neuronal, muscle, and bone cells from human mesenchymal stem cells by culturing them in gels of varying elastic modulus.⁴⁰ Variation in gel stiffness is generally done by varying the concentration of gelator.⁴¹ However, it has been reported that mechanical rigidity can be increased by adding hydrophobic amino acids in the peptide sequence, or by creating chemical cross-linking through oxidation of cysteine side chains or by using multicomponent systems.⁴²

The comprehensive goal of this work was to develop a cheap, noncytotoxic, nanofibrous hydrogel, which can act as a scaffold for adherence and proliferation of cells. We demonstrate that it is possible to regulate gel stiffness (mechanical strength) and thermal stability by incorporating different dicarboxylic acids (oxalic acid, succinic acid, glutaric acid and octanedioic acid) as they promote extended noncovalent interaction between the histidine containing, N-termini free peptide molecules. By tuning the elasticity of dicarboxylic acid incorporated peptide hydrogel through the variation of gelator concentration and chain length of dicarboxylic acids, a successful scaffold for mammalian fibroblast cell culture has been achieved. Among all the acids tested, succinic acid leads to the highest gel thermal stability and mechanical stiffness at a given concentration, thus peptide-succinic acid hydrogels at physiological pH (7.5) have been selected as our material of choice. Interestingly, it has been observed that the extended interaction through succinic acid spacer changes the morphology of the hydrogel to a nanofibrous one, which mimics the extracellular matrix protein more than the native peptide gel with a nanospherical morphology. In this study, 3D cell culture was possible in the hydrogel with a storage modulus of 4 kPa, whereas for a stiffer gel with storage modulus of 9.7 kPa, only 2D culture was possible on the surface of the hydrogel. Thus, a two-component hydrogel with a suitable gel stiffness can serve as a successful cell culture scaffold for mouse fibroblasts and this holds future promise in the field of short peptide-based regenerative medicine and tissue engineering.

MATERIALS AND METHODS

Chemicals and Cell Line. 11-Aminoundecanoic acid was purchased from Sigma-Aldrich. L-Histidine, L-isoleucine, DCC, hydroxybenzotriazole (HOBt), NaOH, chloroform, methanol, silica gel (100–200 mesh), Et₂O, petroleum ether, EtOAc, and DMF were purchased from SRL (India). Formic acid, succinic acid, oxalic acid dihydrate, sodium dihydrogen phosphate, and disodium hydrogen phosphate were purchased from Merck. Glutaric acid and octanedioic acid were obtained from Spectrochem Pvt. Ltd. The water used in all experiments was Millipore Milli-Q grade. Dulbecco's modified Eagle medium (DMEM) supplemented with 10% fetal bovine serum (FBS), penicillin, and streptomycin were procured from Himedia, NIH-3T3 cells were from ATCC.

Synthesis and Characterization of Peptide. The tripeptide was synthesized by conventional solution phase methods by using a racemization-free fragment condensation strategy. All steps of the

synthetic details are provided in the [Supporting Information](#). The final compound was fully characterized by mass spectrometry, ¹H NMR spectroscopy and ¹³C NMR spectroscopy. All NMR studies were carried out on a Bruker DPX 400 MHz or Bruker DPX 500 MHz spectrometer at 300 K. Concentrations were in the range 5–10 mmol in CDCl₃ or DMSO-*d*₆. Mass spectra were recorded on a Q-Tofmicro (Waters Corporation) mass spectrometer by positive mode electrospray ionization process.

Transmission Electron Microscopy (TEM) Study. The morphology of the hydrogel was investigated by using a transmission electron microscope. The samples were prepared by depositing 10 μL of gel sample (0.002% w/v in the case of dilute sample and 0.01% w/v for concentrated ones) onto a TEM grid (300 mesh Cu grid). After 2 min excess fluid was soaked. Then, the grid was dried under vacuum at 27 °C for 12 h. Images were recorded on a JEOL electron microscope at an accelerating voltage of 200 kV.

Fourier Transform Infrared (FTIR) Study. Fourier transformed Infrared spectroscopy study of the xerogels were done in the solid state (KBr matrix) using a Nicolet 380 FT-IR spectrophotometer (Thermo Scientific).

Powder X-ray Diffraction (XRD) Study. The low-angle X-ray (scans over 2θ = 0.6–5°) diffraction studies of xerogels were carried out using an X-ray diffractometer (Bruker AXS, Model D8 Advance). The instrument was operated at a 40 kV voltage and 40 mA current using Ni-filtered CuKα radiation and the instrument was calibrated with a standard Al₂O₃ (corundum) sample before use. The scintillation counts detector was used with scan speed 2s and step size 0.02°. For wide-angle X-ray (For scans over 2θ = 10–50°) diffraction studies, the same samples were studied under a Rigaku SmartLab X-ray diffractometer operated at 9 kW (45 kV, 200 mA) using Ni filtered CuKα radiation and a 1D detector with scan speed 0.3 s and step size 0.02°. Samples were prepared by freeze-drying the hydrogels.

Small-Angle X-ray Scattering (SAXS). Simultaneous SAXS/WAXS experiments were performed at the NCD station of the ALBA synchrotron (Cerdanyola del Vallès, Spain). The sample-to-SAXS detector distance was ca. 2592 mm using a wavelength of 0.998 Å. A Dectris-Pilatus 1 M detector was used to record the 2D SAXS patterns. Standard corrections for sample absorption and background subtraction were performed. The data were normalized to the intensity of the incident beam (to correct for primary beam intensity fluctuations) and were corrected for absorption and background scattering. The scattering patterns from AgBe were used to calibrate the wavevector scale of the scattering curve. WAXS patterns were collected using a Rayonix Lx 255-HS detector at a distance of 135 mm from the sample. The wavenumber $q = 4\pi/\lambda \sin \theta$ scale for WAXS experiments was calibrated using corundum.

Cell Culture and Microscopy. Custom made 35 mm plastic Petri dishes, with a concentric hole of diameter 10 mm, were fitted with 22 × 22 mm glass coverslips on the bottom using biocompatible silicone grease. A sterile rubber O-ring of diameter 12 mm was attached on top of the hole, also using silicone grease, creating a cylindrical enclosure of height ~3 mm. Then 100 μL of the gel, preheated to the sol state, was poured onto the glass inside the hole and allowed to cool down and solidify. NIH 3T3 cells, cultured at 37 °C/5% CO₂, in Dulbecco's modified Eagle medium (DMEM), supplemented with 10% fetal bovine serum (FBS), 100 units/ml of penicillin, and 100 μg/mL of streptomycin were grown up to 85–90% confluence, and then harvested using 0.5 mM EDTA. 1 × 10⁴ cells suspended in 100 μL of culture media were seeded on the gel only inside the space enclosed by the O-ring, and the dish was kept undisturbed for at least 10 min to allow the cells to settle. The dish was then filled with 3 mL of culture medium and stored in the cell culture incubator. Cells were then observed every 6 h using an inverted microscope (Zeiss AxioObserver Z1). Images were taken at 40x and 20x magnification using a CMOS camera (Hamamatsu Orca Flash 4.0 V2). Cells were stained with Hoechst 3342 to visualize the nucleus. Rhodamine 123 was used to stain the live cells. Hoechst 3342 and Rhodamine 123 solutions were prepared as 1 μg/mL and 10 μg/mL to stain the cells.

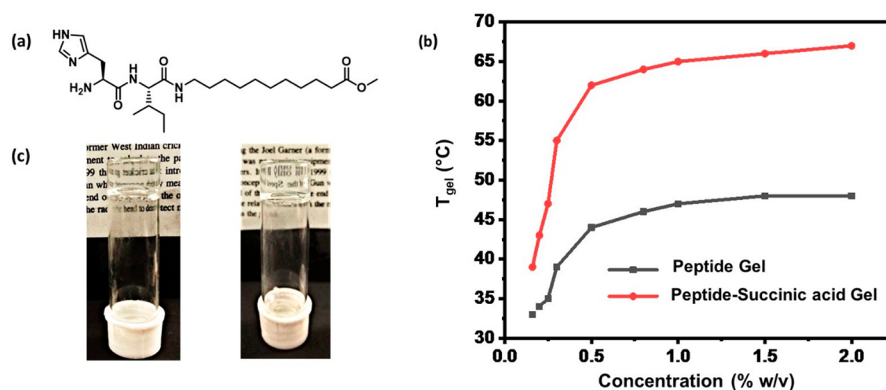


Figure 1. (a) Chemical structure of peptide **P1**; (b) gel melting temperature (T_{gel}) of hydrogel obtained from **P1** and hydrogel obtained from **P1** added with succinic acid, plotted against various concentrations; (c) inverted vial images of peptide gel (left) and peptide-succinic acid gel (right).

MTT Assay. An MTT assay⁴³ was performed to assess the viability of cells in the hydrogel environment. Mitochondrial active succinate dehydrogenase converts MTT (3-[4,5-dimethylthiazol-2-yl]-2,5-diphenyl tetrazolium bromide) into purple colored formazan crystals, and its absorbance at 570 nm is proportional to the number of live cells. Ten thousand cells were seeded for 48, 36, 24, and 12 h from the time of addition of the MTT in a 48-well plate, with or without hydrogel. Gels of two different concentrations (1% and 2% w/v) were used to assess the effect of 2D and 3D environment on cell proliferation. Cells in each well were simultaneously treated with MTT (0.5 mg/mL) for 3 h at 37 °C/5% CO₂. After incubation, 200 μ L of DMSO was added to each well and absorbance at 570 nm was measured on a SpectraMax M2 spectrometer (Molecular Devices). Each condition was repeated thrice and errors bar representing standard deviation are plotted as part of the assessment of cell viability in the hydrogel environment, with the cells grown in standard poly-L-lysine-coated plastic surface as control.

RESULTS AND DISCUSSION

The L-histidine containing C-terminal protected tripeptide NH₂-His-Ile-AUDA-COOMe (AUDA = 11-aminoundecanoic acid) **P1** (Figure 1a) was synthesized in solution phase and subsequently purified and characterized.

Gelation Study. The gelation property of **P1** was tested in the full spectrum of pH of phosphate buffer solutions (PBS) and it was found that a transparent hydrogel was formed between pH 5.5 and 8.5. For each gelation study, 4 mg of the solid peptide was taken in a glass vial and dissolved in 1 mL of PBS by heating with a hot-gun until a clear solution was obtained. The solution was allowed to equilibrate at room temperature (27 °C) and it turned translucent as it was cooled down within 60 s. Interestingly, it became transparent as hydrogel formation took place. The gel melting temperature of the peptide hydrogel at pH 7.46 was found to be 44 °C (0.5% w/v, i.e., 10.75 mM). To strengthen the network of the hydrogel, we have incorporated various dicarboxylic acids into the peptide gel network. For each gelation experiment 4 mg (8.6 μ mol) of solid peptide was placed in 950 μ L of PBS (pH 7.46), dissolved by careful heating with a hot-gun and 50 μ L of 85 mM (4.3 μ mol) dicarboxylic acid solution (oxalic acid, succinic acid, glutaric acid and octanedioic acid) was added to it to obtain the peptide-dicarboxylic acid based two-component hydrogels. There was no significant change in the appearance of the gel as the pH changed from 5.5 to 8.5 (Figure S11), and the addition of dicarboxylic acid of different chain length did not show any significant change in the appearance of two-component hydrogels (Figure S11). It was

observed that the gel melting temperature significantly increased upon the addition of dicarboxylic acids (Table S2). The most prominent improvement was shown for peptide-succinic acid gel, which showed a T_{gel} of 62 °C (0.5% w/v). The native hydrogel, as well as the gels obtained after the addition of succinic acid, were found to be transparent and suitable for microscopic studies (Figure 1c). A comparative study of gel melting temperature versus concentration of gelator, between native peptide gel and the peptide-succinic acid gel, shows the improvement of thermal stability over all concentration range. It is noted that T_{gel} values become essentially independent of concentration above 1% w/v for both the hydrogels (Figure 1b).

Morphology. High-resolution transmission electron microscopic (HR-TEM) studies were performed to examine the morphologies of the gelators in different assembled states (aggregated nongel and gel states). Samples of **P1** hydrogels were made at two different concentrations to understand the nature of the aggregation. The HR-TEM images obtained from the dilute solution reveals the formation of nanospheres (Figure 2a). The radii of the nanospheres vary from 80 to 100 nm. The radii are plotted in a frequency distribution histogram (Figure S10a) and the average radius is found to be 90 nm. In the nongel state, the nanospheres are obtained from the aggregation of gelator molecules and these nanospheres are aligned in a regular fashion forming a network-like arrangement (Figure 2b). Although this is a rare phenomenon, a few examples have been observed for the spherical morphology in gels formed by assembly of small molecules.^{44,45} The three-dimensional porous network structure formed by adhered interconnecting nanospheres shows a beads-on-a-string-like morphology in the concentrated gel phase (Figure 2c). This cagelike porous structure can entrap a lot of water molecules into it to form a self-supporting hydrogel. Interestingly, a change in the morphology is observed in the two-component gel consisting of the peptide gelator **P1** and succinic acid. In presence of the acid, a well-resolved interconnected helical nanofibrous network structure is obtained (Figure 2d). The width of the gel forming fibers ranges from 40 to 60 nm. A histogram showing frequency distribution of widths (Figure S10b) of different fibers reveals that the average width of the fibers is 50 nm. Widths of most of these fibers lie within the range from 50 to 55 nm. The network shows the presence of both right and left-handed helicity (Figure 2e). The nanofibrous network is well adapted to support the proliferation of mammalian cells. The images reveal a remarkable transition

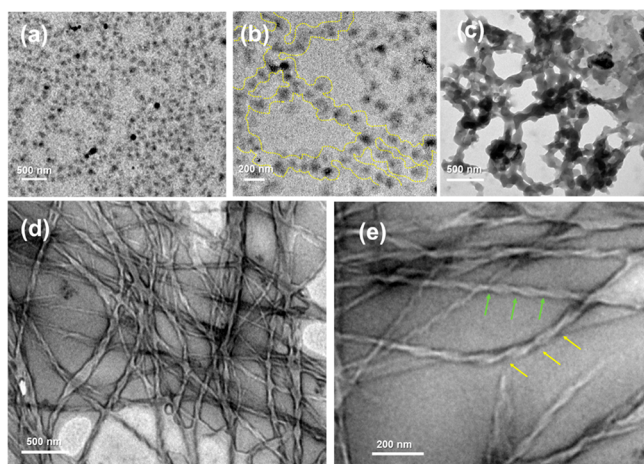


Figure 2. High-resolution transmission electron microscopic images showing (a) nanospheres composing the peptide hydrogel; (b) magnified image of the nanospheres arranged in a network-like arrangement (yellow dotted line highlights the pattern); (c) 3D network assembly of the nanospheres showing beads-on-a-string-like morphology; (d) helical fibrous morphology of peptide-succinic acid hydrogel, (e) Individual fibers of peptide-succinic acid gel. (Green arrows and yellow arrows show two different kinds of handedness in the helices.)

from a nanosphere (soluble aggregated nongel state) to a beads-on-a-string morphology in the gel state. A few previous reports describe morphological transformations within hydrogel systems.^{46–48} However, it is rare to observe a drastic change in morphology (interconnected nanospheres to helical

nanofibers) from one gel phase (only peptide) to another gel phase (peptide + succinic acid).

Fourier-Transform Infrared (FT-IR) Spectroscopic Study. Intense peaks at 3291 cm^{-1} corresponding to N–H stretching vibration, 1637 cm^{-1} corresponding to amide C=O stretching (amide I), and 1555 cm^{-1} (N–H bending) suggest a strongly hydrogen-bonded network in the P1 hydrogel at physiological pH (Figure S4).⁴⁹ Similar kind of IR signatures were found in two component gels with various dicarboxylic acids. Moreover, the decrease in the stretching frequency of ester C=O to 1730 cm^{-1} suggests bond elongation, which indicates its participation in hydrogen bonding (the ester C=O stretching generally appears within the $1735\text{--}50\text{ cm}^{-1}$ range).⁵⁰ A xerogel obtained from the two-component gel containing peptide and succinic acid shows symmetric and antisymmetric stretching of carboxylate anion of succinic acid at 1420 and 1570 cm^{-1} , respectively along with the other peaks observed for the peptide-only gel (Figure S4).

Powder X-ray Diffraction Studies. To probe the molecular packing within the gels, X-ray diffraction studies of powdered freeze-dried gels were performed. In the low angle diffraction pattern, for the peptide only gel, we observed a peak at $D = 30.26\text{ \AA}$ ($2\theta = 2.84^\circ$), which can be attributed to the length of two peptide molecules interdigitated along the hydrocarbon chain (Figure 3a) (Estimated molecular length of P1 is 24.62 \AA). A similar packing was reported previously for a lipidated histidine dipeptide gelator.⁵¹ In the wide-angle diffraction patterns, peaks at 4.78 \AA ($2\theta = 18.05^\circ$) are ascribed to the distance between β -strands and the peak at 9.87 \AA ($2\theta = 8.71^\circ$) corresponds to the distance between two stacked β sheets (Figure 3b).⁵² Interestingly four peaks at 5.48 \AA ($2\theta = 15.72^\circ$), 4.39 \AA ($2\theta = 19.66^\circ$), 3.74 \AA

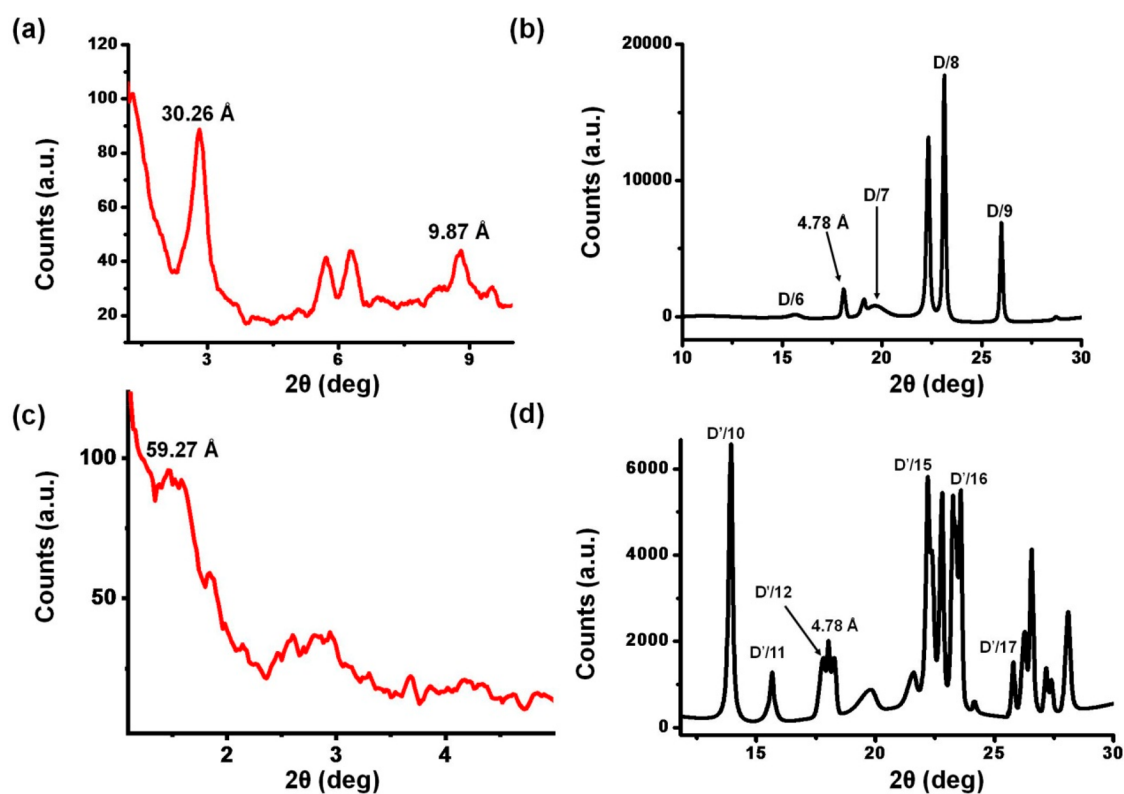


Figure 3. (a) Low-angle, (b) wide-angle X-ray diffraction pattern recorded for xerogel obtained from peptide hydrogel. (c) Low-angle, (d) wide-angle X-ray diffraction pattern recorded for xerogel obtained from succinic acid peptide hydrogel.

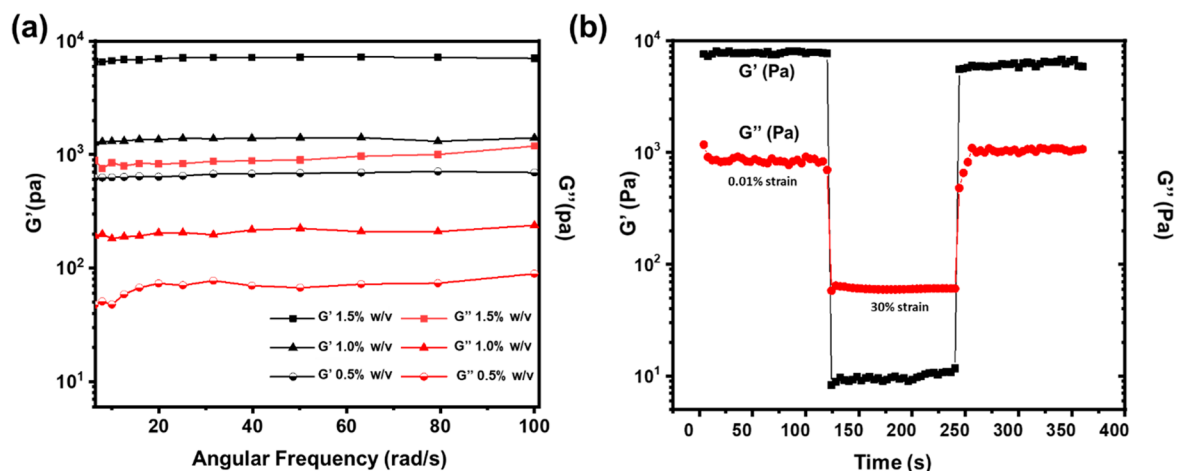


Figure 4. (a) Elastic modulus G' and Loss modulus G'' of hydrogels of peptide P1 in three different concentrations 1.5, 1, and 0.5% w/v; (b) step strain experiment for 1.5% w/v of peptide P1 hydrogel with 125 s step length, confirming thixotropic behavior of the hydrogel.

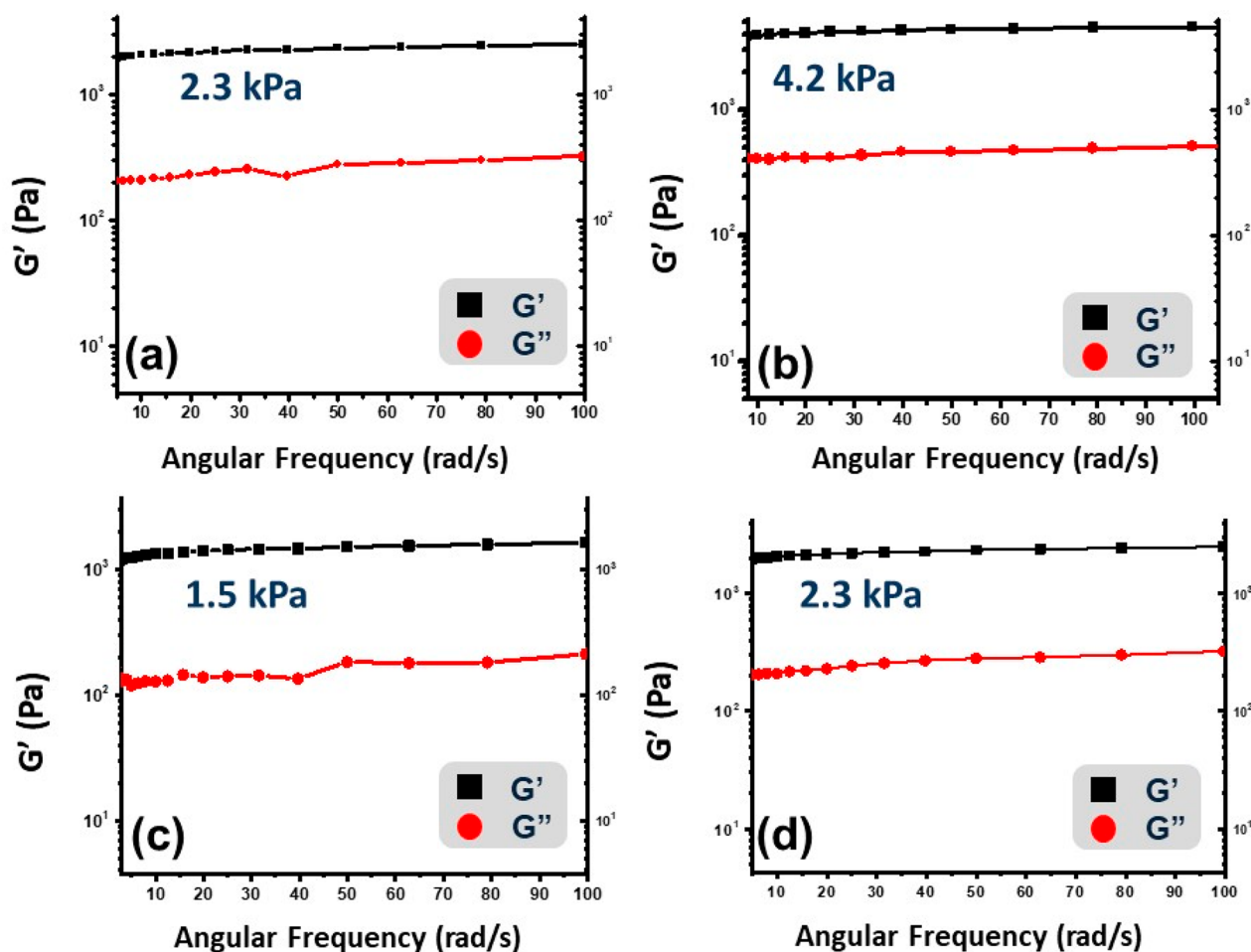


Figure 5. Elastic modulus G' and loss modulus G'' of hydrogels of peptide P1 with different additives: (a) oxalic acid, (b) succinic acid, (c) glutamic acid, (d) octanedioic acid, with value of G' at 50 rad/s indicated for each case. Peptide and dicarboxylic acid were taken in a 2:1 molar ratio with 1% (w/v) (21.50 mM) peptide in each hydrogel.

($2\theta = 23.13^\circ$), 3.33 \AA ($2\theta = 26.00^\circ$) correspond to $D/6$, $D/7$, $D/8$, and $D/9$, respectively. This indicates a lamellar type of packing arrangement.⁵² Investigation of small-angle diffraction pattern from succinic acid-peptide xerogels showed a peak at $D' = 59.27 \text{ \AA}$ ($2\theta = 1.45^\circ$). The total molecular length of two peptide molecules and a succinic acid (5.05 \AA) (estimated in

Chem3D Pro 12.0 software) is 54.3 \AA . However, if the succinate anion and the peptide molecules are connected through hydrogen bonding between imidazole N–H and carboxylate O, the overall supramolecular unit length increases by twice that of N–H \cdots O hydrogen-bond length^{53,54} ($2.7 \text{ \AA} \times 2 = 5.4 \text{ \AA}$) and it becomes 59.69 \AA , which is in accordance with

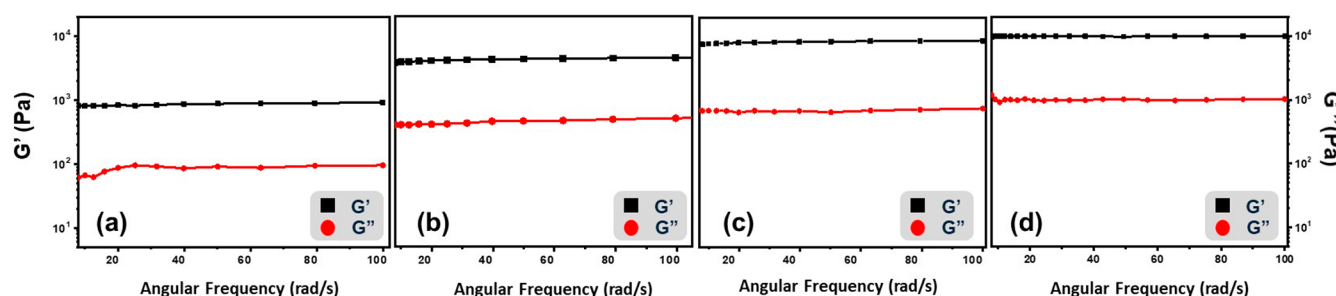


Figure 6. Elastic modulus G' and loss modulus G'' of hydrogels of two component gel of peptide and succinic acid in different concentrations of peptide and succinic acid: (a) 0.5, (b) 1, (c) 1.5, and (d) 2% w/v.

the d -spacing found by XRD (Figure 3c). So, we can conclude that the two peptide molecules are interconnected by a centrally located succinic acid moiety through hydrogen bonding. Furthermore, three peaks at 6.13 Å ($2\theta = 14.05^\circ$), 5.50 Å ($2\theta = 15.67^\circ$), 4.85 Å ($2\theta = 17.81^\circ$) can be interpreted as $D'/10$, $D'/11$, and $D'/12$, and this suggests the length corresponding to two terminally located peptide molecules hydrogen-bonded to a centrally positioned succinic acid moiety (Figure 3d). Another set of peaks was found at 3.90 Å ($2\theta = 22.22^\circ$), 3.66 Å ($2\theta = 23.62^\circ$), 3.36 Å ($2\theta = 25.82^\circ$), assigned as $D'/15$, $D'/16$ and $D'/17$. It shows that the peptide-succinic acid gel packs in a lamellar fashion. Again, the d -spacing of 4.78 Å ($2\theta = 18.05^\circ$) is the distance between β -strands.

Small-Angle X-ray Scattering (SAXS) Study. To visualize single molecular length and mode of packing of the peptide in the (undried) gel state, we carried out small-angle X-ray scattering (SAXS). The d -spacing of 30.2 Å (Figure S5) can be assigned to the length of a layered structure of two interdigitated peptides. These data support the low-angle powder XRD data of the dried peptide gel. On the basis of SAXS and PXRD and FT-IR studies, probable models for the molecular packing pattern of the gel phase has been constructed in Figures S6 and S7 for the native peptide gel and the two-component gel (obtained from peptide and succinic acid), respectively.

Rheological Study. The stiffness of the extracellular matrix is known to influence cell physiology, and thus, it is a crucial parameter to address when developing hydrogels as models for tissue systems. The degree of stiffness of the peptide hydrogels and peptide-dicarboxylic acid gels were systematically measured and compared to get an insight into how the incorporation of these acids affects the mechanical strength of the native gel. Time sweep rheology data of the peptide gel was also recorded to quantify the visible thixotropic property of the hydrogel. First, the frequency sweep experiment was done for peptide hydrogel with gelator concentration 0.5% (w/v) (10.75 mM) where the two moduli, i.e., storage modulus (G') and loss modulus (G'') were plotted against angular frequency (ω) ranging from 8 to 100 rad/s, at a constant strain of 0.1%. The moduli show an insignificant dependence on angular frequency (Figure 4A). This indicates the formation of a stable gel. To attain higher stiffness, we increased the concentration of the gelator to 1.0% w/v (21.50 mM) and 1.5% w/v (32.25 mM). Doubling the concentration of the peptide increased the elastic modulus by a factor of 2, whereas tripling the concentration increased the elastic modulus 10-fold. At $\omega = 50$ rad/s, G' is 690, 1402, and 7006 Pa for 0.5, 1, and 1.5% w/v hydrogel, respectively (Figure 4a). The time-

dependent step-strain experiment was performed with a time step of 125 s. Initially, the strain was kept constant at 0.1% then the strain was increased to 30%, at which point the gel ruptured. The reformation of the gel takes place as the strain is reduced to 0.1% at the next cycle. The process was continued to 3 cycles to show reproducibility (Figure 4b).

Dicarboxylic acids with varying chain lengths were incorporated with an expectation of extended supramolecular interactions between free carboxylic acid groups and peptide molecules with free N terminus, as well as the imidazole side chain of the histidine residue. Peptide-dicarboxylic acids at 1% w/v (21.50 mM) concentration of peptide and acids taken in 2:1 molar ratios indeed showed increased storage modulus, to different degrees, for different acids (Figure 5).

The most significant enhancement of mechanical strength was shown by the addition of succinic acid (Figure 5). Because of its optimal mechanical and thermal response, the transparent gels of peptide-succinic acid were used in cell culture. Stiffness tuning of the peptide-succinic acid gel could be achieved by varying the concentration from 0.5% to 2.0% w/v (Figure 6). At $\omega = 50$ rad/s, G' is 879 Pa, 4340, 8357, and 9729 Pa for 0.5, 1, 1.5, and 2% w/v hydrogel, respectively. A step strain experiment was also performed for peptide-succinic acid hydrogel (Figure S8) to confirm the thixotropic behavior which was observed visually. The reformation of gel phase takes place within 30 min.

Cell Culture Experiments. The histidine-based hydrogel is optically transparent, and it forms gels at a physiological pH of 7.5. Free NH_2 groups give it a net positive charge at pH 7.5, which would facilitate adhesion of negatively charged cell membranes on the substrate. Moreover, the stiffness of the gel can be tuned by varying the gelator concentration. This makes our hydrogel system a good candidate as an extracellular matrix mimic. Because of transparency and good rheological response, the hydrogel of P1 was initially used to investigate whether cells can grow on them or not. The fibroblast cell line NIH 3T3 was employed for cell culture experiments. Cell culture was attempted on the peptide gel (1.5% w/v) (32.25 mM) with the stiffness of 7 kPa, but it was found that the gel would disappear readily within 6 h at the incubator temperature of 37 °C. This is because the gel melting temperature of the pure peptide gel at 1.5% w/v gelator concentration is 48 °C and this makes it slightly unstable at the physiological temperature of 37 °C. To primarily increase the thermal stability of the hydrogel, we incorporated several dicarboxylic acids along with the peptide gelator. As detailed above, the peptide-succinic acid gel gave the best thermal and mechanical response. The nanofibrous morphology of the peptide-succinic acid gel also encouraged us to investigate its possibility of acting as an

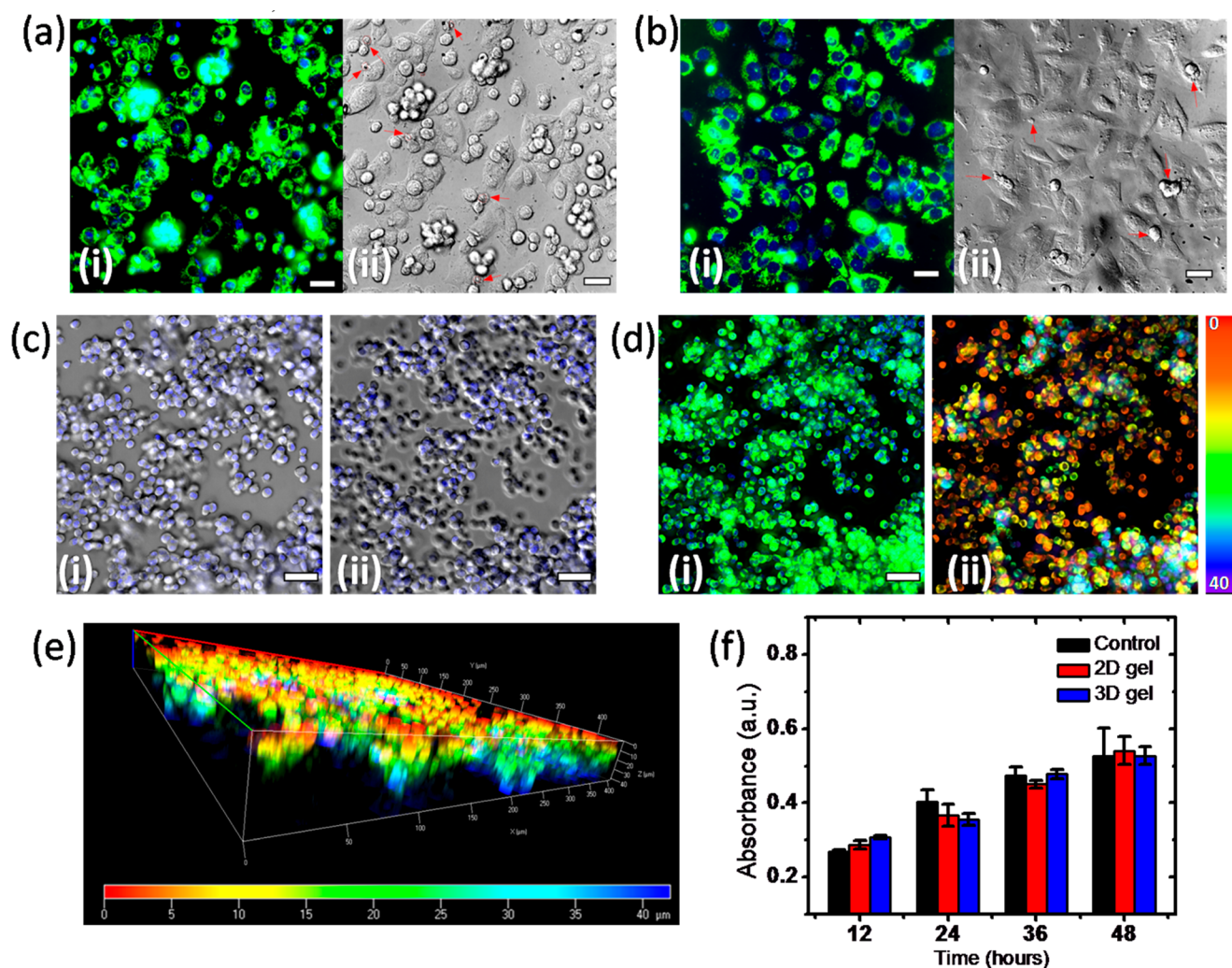


Figure 7. (a) (i) Fluorescence image of Rhodamine 123 (green) and Hoechst (blue) stained NIH 3T3 cells cultured on the surface of 2% (w/v) gel and (ii) the corresponding differential interference contrast (DIC) image (40 \times magnification) at 36 h post seeding. Dead cells do not get stained by Rhodamine 123, so having their nuclei stained by Hoechst, they appear only blue. Dead cells have been pointed out in the DIC image using red arrows. (b) (i) Fluorescence and (ii) DIC image of cells grown on glass at 36 h post seeding. Upon culturing cells on 1% (w/v) hydrogel, it was observed that cells were present at different depths inside the gel, post 36 h of seeding the cells on the surface. (c) (i) DIC images (20 \times magnification) with the cell nuclei stained with Hoechst (blue) on the surface of the gel, (ii) cells at a depth of 20 μm inside the gel. (d) (i) Maximum intensity projection of fluorescence images of Rhodamine123/Hoechst stained cells at 22 focal planes spanning a depth of 40 μm . (ii) Cells having Rhodamine 123 fluorescence were color coded according to their depth inside the gel in the maximum intensity projection, with red indicating the gel surface. (e) 3D Volume Rendering of Rhodamine 123 stained cells (color bar indicates location of cell in the Z direction). (f) MTT assay comparing viability of cells on glass surface (black), 2% (w/v) gel for 2D culture (red), and 1% (w/v) gel for 3D culture (blue). Scale bars in a and b indicate 30 μm , and those in c and d indicate 50 μm .

extracellular matrix for cell growth and proliferation. Cell culture was performed on custom-made glass bottomed Petri dishes. Cell culture was first attempted on 2% w/v (43 mM peptide in peptide-succinic acid gel ($G' = 9.7$ kPa). Cell growth was monitored for 36 h at 6 h intervals, after which the gel mass generally got detached from the glass surface, making microscopy difficult. Figure 7a shows that the cells are able to grow on the two-component peptide-based gel surface for at least 36 h without any debilitating effect on viability. Cells did not exhibit a well-spread morphology, possibly due to the absence of stable focal adhesions.^{55–57} Fibroblasts are also known to tune their internal stiffness to enable survival and proliferation on substrates with lower stiffness, which often results in a rounded morphology.^{58,59} The cells that did have elongated morphology could have secreted ECM proteins (locally) as typical of fibroblasts⁶⁰ (Figure 7a). When cells

were cultured on a lower concentration 1% w/v gel of a lower $G' = 4$ kPa, it was convincingly apparent that they could penetrate deep inside the gel (Figure 7c–e). To assess their viability, the cells were stained with Rhodamine 123, a green fluorescent dye that accumulates on respiring mitochondrial membrane. Cell nuclei were also stained with the blue fluorescent dye, Hoechst. Live cells exhibit both green and blue fluorescence, while dead cells without respiring mitochondria just have only blue fluorescence. In Figure 7a, b, the Rhodamine 123/Hoechst staining reveals the living and dead cells cultured on 2% (w/v) hydrogel and glass. Figure 7a–ii and b–ii have the dead cells indicated with red arrows. It is known that contractile forces generated by cells on the culture substrate can influence the mechanical architecture of the substrate.⁶¹ In the case of the P1-succinic acid gel, the cellular traction stress could have broken the gel in a localized manner,

thus enabling the cells to travel inside by constantly dissolving the gel beneath them. The gel above the cells could then recover from solution state to reform the gel after some time because of its thixotropic property. Figure 7c shows DIC images of cells grown on the surface of the 1% w/v hydrogel. General cell morphology is rounder than the cells cultured on the 2% w/v, but Rhodamine 123/Hoechst staining Figure 7d shows that cells are alive and healthy post 36 h after seeding on the gel. By imaging the Rhodamine 123 fluorescence of cells at 22 focal planes starting from the gel surface, each plane being 2 μm apart, a 2D maximum intensity projection of the 3D fluorescence was generated, which essentially means showing only the brightest pixel of a 3D voxel (Figure 7d-i). Depth color coding of the maximum intensity projection image reveals the distribution of the live cells along the height of the gel (Figure 7d-i), which is reiterated by the 3D volume rendering (Figure 7e) of the Rhodamine 123 stained cells. An MTT cell survival assay was performed to examine the influence of peptide-succinic acid hydrogel on cell viability over time. The assay reveals that the 2D or 3D environment provided by the peptide gel has no detrimental effect on cell viability (Figure 7f). This indicates that the peptide-based hydrogel obtained from gelator P1 and succinic acid is not cytotoxic, and it can be used to mimic the extracellular matrix to culture fibroblasts in vitro up to 2 days at least. We also did the cell growth experiments with the cell line RAW264.7 murine macrophages. This suggests that the hydrogel based biomaterial is a good support for the growth of different types of cells in vitro. Details of that study can be found in the Figure S12.

The aforementioned study suggests that the tuning of the thermal stability of the hydrogel enhances the gel stability for a sufficiently long time that is needed for the cell culture. Moreover, the mechanical stiffness of the hydrogel can be modulated according to the traction stress generated by the cell type to choose the culture environment as 2D or 3D. Relatively less stiff gel ($G' = 4$ kPa) is well-suited for 3D culture, as it promotes selective penetration of cells into the gel phase material, whereas increasing the gel stiffness above the cellular traction stress provides a platform for 2D culture on the hydrogel surface. Here, gel stiffness was optimized for successful culture of NIH-3T3 cells in 2D and 3D environments.

CONCLUSION

We demonstrated the formation of a histidine-containing peptide-based hydrogel at pH 7.5. This study also convincingly demonstrates the tuning of mechanical stiffness and thermal stability of this peptide-based supramolecular hydrogel by incorporation of different dicarboxylic acids into the system, promoting hydrogen bonding and electrostatic interaction within the gel phase. We show for the first time that it is possible to improve the thermal and mechanical properties of a peptide hydrogel by introducing a dicarboxylic acid (succinic acid in 1:2 molar ratio) to promote acid base interaction in a two-component hydrogel system. Interestingly, the morphology of the native gel changes significantly in the presence of succinic acid from bead-on-a-garland to a network of interconnected helical nanofibers to form a two component hydrogel. The increased gel stiffness, the enhanced gel melting temperature, and a nanofibrous network have been successfully utilized for the 3D/2D culture of fibroblasts by using the two-component hydrogel as an extracellular matrix. This indicates

that the tuning of mechanical strength, thermal stability and the morphology of the hydrogel promotes growth and nourishment of the cells in vitro pointing toward the future promise for peptide gel-based soft biomaterials in regenerative medicine.

ASSOCIATED CONTENT

Supporting Information

The Supporting Information is available free of charge on the ACS Publications website at DOI: 10.1021/acsabm.9b00424.

Synthetic procedure, FT-IR spectra analysis, SAXS data, hydrogels' specifications, tentative model of the self-assembly, thixotropic behavior of two-component gel, hydrogel images, RAW264.7 murine macrophages cell culture (PDF)

AUTHOR INFORMATION

Corresponding Author

*Email: bcab@iacs.res.in (A.B.).

ORCID

Ian W. Hamley: 0000-0002-4549-0926

Arindam Banerjee: 0000-0002-1309-921X

Notes

The authors declare no competing financial interest.

ACKNOWLEDGMENTS

D.B. and S.H. gratefully acknowledge UGC for their research fellowship. P.B. and K.B thank IACS for the financial support. We acknowledge Dr. P. Sen for being kind enough to donate us the MTT reagent. We also thank Professor Kumar Biradha and his student Mr. Rajib Moi and, Mr. Krishna S. Das for carrying out the rheology experiments. IWH thanks EPSRC for the award of a Platform Grant (EP/L020599/1) and DH-M thanks ALBA (Cerdanyola del Vallès, Spain) for the award of synchrotron beamtime.

REFERENCES

- (1) Dou, X.-Q.; Feng, C.-L. Amino Acids and Peptide-Based Supramolecular Hydrogels for Three-Dimensional Cell Culture. *Adv. Mater.* **2017**, *29*, 1604062.
- (2) Raeburn, J.; Adams, D. J. Multicomponent Low Molecular Weight Gelators. *Chem. Commun.* **2015**, *51*, 5170–5180.
- (3) Hirst, A. R.; Escuder, B.; Miravet, J. F.; Smith, D. K. High-Tech Applications of Self-Assembling Supramolecular Nanostructured Gel-Phase Materials: From Regenerative Medicine to Electronic Devices. *Angew. Chem., Int. Ed.* **2008**, *47*, 8002–8018.
- (4) Datta, S.; Dey, N.; Bhattacharya, S. Electrochemical Probing of Hydrogelation Induced by the Self-assembly of a Donor–Acceptor Complex Comprising Pyranine and Viologen. *Chem. Commun.* **2017**, *53*, 2371–2374.
- (5) Panda, S. S.; Katz, H. E.; Tovar, J. D. Solid-State Electrical Applications of Protein and Peptide Based Nanomaterials. *Chem. Soc. Rev.* **2018**, *47*, 3640–3658.
- (6) Kumar, M.; Ing, N. L.; Narang, V.; Wijerathne, N. K.; Hochbaum, A. I.; Ulijn, R. V. Amino-Acid-Encoded Biocatalytic Self-Assembly Enables the Formation of Transient Conducting Nanostructures. *Nat. Chem.* **2018**, *10*, 696–703.
- (7) Lampel, A.; Ulijn, R. V.; Tuttle, T. Guiding Principles for Peptide Nanotechnology through Directed Discovery. *Chem. Soc. Rev.* **2018**, *47*, 3737–3758.
- (8) Hellmund, K. S.; Koks, B. Self-Assembling Peptides as Extracellular Matrix Mimics to Influence Stem Cell's Fate. *Front. Chem.* **2019**, *7*, 172.

- (9) Li, Y.; Wang, F.; Cui, H. Peptide-Based Supramolecular Hydrogels for Delivery of Biologics. *Bioeng. Transl. Med.* **2016**, *1*, 306–322.
- (10) Sato, K.; Hendricks, M. P.; Palmer, L. C.; Stupp, S. I. Peptide Supramolecular Materials for Therapeutics. *Chem. Soc. Rev.* **2018**, *47*, 7539–7551.
- (11) Sahoo, J. K.; Braegelman, A. S.; Webber, M. J. Immunoengineering with Supramolecular Peptide Biomaterials. *J. Indian Inst. Sci.* **2018**, *98*, 69–79.
- (12) Qi, G.-B.; Gao, Y.-J.; Wang, L.; Wang, H. Self-Assembled Peptide-Based Nanomaterials for Biomedical Imaging and Therapy. *Adv. Mater.* **2018**, *30*, 1703444.
- (13) Stern, D.; Cui, H. Crafting Polymeric and Peptidic Hydrogels for Improved Wound Healing. *Adv. Healthcare Mater.* **2019**, *8*, 1900104.
- (14) Carrejo, N. C.; Moore, A. N.; Lopez Silva, T. L.; Leach, D. G.; Li, I.-C.; Walker, D. R.; Hartgerink, J. D. Multidomain Peptide Hydrogel Accelerates Healing of Full-Thickness Wounds in Diabetic Mice. *ACS Biomater. Sci. Eng.* **2018**, *4*, 1386–1396.
- (15) Wei, Q.; Duan, J.; Ma, G.; Zhang, W.; Wang, Q.; Hu, Z. Enzymatic Crosslinking to Fabricate Antioxidant Peptide-Based Supramolecular Hydrogel for Improving Cutaneous Wound Healing. *J. Mater. Chem. B* **2019**, *7*, 2220–2225.
- (16) Koch, F.; Wolff, A.; Mathes, S.; Pieleus, U.; Saxer, S. S.; Kreikemeyer, B.; Peters, K. Amino Acid Composition of Nanofibrillar Self-Assembling Peptide Hydrogels Affects Responses of Periodontal Tissue Cells in Vitro. *Int. J. Nanomed.* **2018**, *13*, 6717–6733.
- (17) Kisiday, J.; Jin, M.; Kurz, B.; Hung, H.; Semino, C.; Zhang, S.; Grodzinsky, A. J. Self-Assembling Peptide Hydrogel Fosters Chondrocyte Extracellular Matrix Production and Cell Division: Implications for Cartilage Tissue Repair. *Proc. Natl. Acad. Sci. U. S. A.* **2002**, *99*, 9996–10001.
- (18) Wang, H.; Yang, Z. Short-Peptide-Based Molecular Hydrogels: Novel Gelation Strategies and Applications for Tissue Engineering and Drug Delivery. *Nanoscale* **2012**, *4*, 5259–5267.
- (19) Tibbitt, M. W.; Anseth, K. S. Hydrogels as Extracellular Matrix Mimics for 3D Cell Culture. *Biotechnol. Bioeng.* **2009**, *103*, 655–663.
- (20) Nandi, N.; Gayen, K.; Ghosh, S.; Bhunia, D.; Kirkham, S.; Sen, S. K.; Ghosh, S.; Hamley, I. W.; Banerjee, A. Amphiphilic Peptide-Based Supramolecular, Noncytotoxic, Stimuli-Responsive Hydrogels with Antibacterial Activity. *Biomacromolecules* **2017**, *18*, 3621–3629.
- (21) Baral, A.; Roy, S.; Ghosh, S.; Hermida-Merino, D.; Hamley, I. W.; Banerjee, A. A Peptide-Based Mechano-Sensitive, Proteolytically Stable Hydrogel with Remarkable Antibacterial Properties. *Langmuir* **2016**, *32*, 1836–1845.
- (22) Salick, D. A.; Pochan, D. J.; Schneider, J. P. Design of an Injectable β -Hairpin Peptide Hydrogel That Kills Methicillin-Resistant *Staphylococcus Aureus*. *Adv. Mater.* **2009**, *21*, 4120–4123.
- (23) Veiga, A. S.; Sinthuvanich, C.; Gaspar, D.; Franquelim, H. G.; Castanho, M. A. R. B.; Schneider, J. P. Arginine-Rich Self-Assembling Peptides as Potent Antibacterial Gels. *Biomaterials* **2012**, *33*, 8907–8916.
- (24) Hu, B.; Owh, C.; Chee, P. L.; Leow, W. R.; Liu, X.; Wu, Y.-L.; Guo, P.; Loh, X. J.; Chen, X. Supramolecular Hydrogels for Antimicrobial Therapy. *Chem. Soc. Rev.* **2018**, *47*, 6917–6929.
- (25) Castelletto, V.; Edwards-Gayle, C. J. C.; Hamley, I. W.; Barrett, G.; Seitsonen, J.; Ruokolainen, J. Peptide-Stabilized Emulsions and Gels from an Arginine-Rich Surfactant-like Peptide with Antimicrobial Activity. *ACS Appl. Mater. Interfaces* **2019**, *11*, 9893–9903.
- (26) Dimatteo, R.; Darling, N. J.; Segura, T. In Situ Forming Injectable Hydrogels for Drug Delivery and Wound Repair. *Adv. Drug Delivery Rev.* **2018**, *127*, 167–184.
- (27) Sun, J. E. P.; Stewart, B.; Litan, A.; Lee, S. J.; Schneider, J. P.; Langhans, S. A.; Pochan, D. J. Sustained Release of Active Chemotherapeutics from Injectable-Solid β -Hairpin Peptide Hydrogel. *Biomater. Sci.* **2016**, *4*, 839–848.
- (28) Raymond, D. M.; Abraham, B. L.; Fujita, T.; Watrous, M. J.; Toriki, E. S.; Takano, T.; Nilsson, B. L. Low Molecular Weight Supramolecular Hydrogels for Sustained and Localized In Vivo Drug Delivery. *ACS Appl. Bio Mater.* **2019**, *2*, 2116–2124.
- (29) Falcone, N.; Kraatz, H. B. Supramolecular Assembly of Peptide and Metallopeptide Gelators and Their Stimuli-Responsive Properties in Biomedical Applications. *Chem. - Eur. J.* **2018**, *24*, 14316–14328.
- (30) Black, K. A.; Lin, B. F.; Wonder, E. A.; Desai, S. S.; Chung, E. J.; Ulery, B. D.; Katari, R. S.; Tirrell, M. V. Biocompatibility and Characterization of a Peptide Amphiphile Hydrogel for Applications in Peripheral Nerve Regeneration. *Tissue Eng., Part A* **2015**, *21*, 1333–1342.
- (31) Arioz, I.; Erol, O.; Bakan, G.; Dikecoglu, F. B.; Topal, A. E.; Urel, M.; Dana, A.; Tekinay, A. B.; Guler, M. O. Biocompatible Electroactive Tetra(Aniline)-Conjugated Peptide Nanofibers for Neural Differentiation. *ACS Appl. Mater. Interfaces* **2018**, *10*, 308–317.
- (32) Koutsopoulos, S. Self-Assembling Peptide Nanofiber Hydrogels in Tissue Engineering and Regenerative Medicine: Progress, Design Guidelines, and Applications. *J. Biomed. Mater. Res., Part A* **2016**, *104*, 1002–1016.
- (33) Matson, J. B.; Stupp, S. I. Self-Assembling Peptide Scaffolds for Regenerative Medicine. *Chem. Commun.* **2012**, *48*, 26–33.
- (34) Yergoz, F.; Hastar, N.; Cimenci, C. E.; Ozkan, A. D.; Tekinay, T.; Guler, M. O.; Tekinay, A. B. Heparin Mimetic Peptide Nanofiber Gel Promotes Regeneration of Full Thickness Burn Injury. *Biomaterials* **2017**, *134*, 117–127.
- (35) Jayawarna, V.; Ali, M.; Jowitt, T. A.; Miller, A. F.; Saiani, A.; Gough, J. E.; Ulijn, R. V. Nanostructured Hydrogels for Three-Dimensional Cell Culture through Self-Assembly of Fluorenylmethoxycarbonyl-Dipeptides. *Adv. Mater.* **2006**, *18*, 611–614.
- (36) Zanna, N.; Focaroli, S.; Merletti, A.; Gentilucci, L.; Teti, G.; Falconi, M.; Tomasini, C. Thixotropic Peptide-Based Physical Hydrogels Applied to Three-Dimensional Cell Culture. *ACS Omega* **2017**, *2*, 2374–2381.
- (37) Worthington, P.; Drake, K. M.; Li, Z.; Napper, A. D.; Pochan, D. J.; Langhans, S. A. Beta-Hairpin Hydrogels as Scaffolds for High-Throughput Drug Discovery in Three-Dimensional Cell Culture. *Anal. Biochem.* **2017**, *535*, 25–34.
- (38) Chakraborty, P.; Guterman, T.; Adadi, N.; Yadid, M.; Brosh, T.; Adler-Abramovich, L.; Dvir, T.; Gazit, E. A Self-Healing, All-Organic, Conducting, Composite Peptide Hydrogel as Pressure Sensor and Electrogenic Cell Soft Substrate. *ACS Nano* **2019**, *13*, 163–175.
- (39) Levental, I.; Georges, P. C.; Janmey, P. A. Soft Biological Materials and Their Impact on Cell Function. *Soft Matter* **2007**, *3*, 299–306.
- (40) Engler, A. J.; Sen, S.; Sweeney, H. L.; Discher, D. E. Matrix Elasticity Directs Stem Cell Lineage Specification. *Cell* **2006**, *126*, 677–689.
- (41) Boothroyd, S.; Saiani, A.; Miller, A. F. Controlling Network Topology and Mechanical Properties of Co-Assembling Peptide Hydrogels. *Biopolymers* **2014**, *101*, 669–680.
- (42) Scelsi, A.; Bochicchio, B.; Smith, A.; Workman, V. L.; Diaz, L. A. C.; Saiani, A.; Pepe, A. Tuning of Hydrogel Stiffness Using a Two-Component Peptide System for Mammalian Cell Culture. *J. Biomed. Mater. Res., Part A* **2019**, *107*, 535–544.
- (43) Mosmann, T. Rapid Colorimetric Assay for Cellular Growth and Survival: Application to Proliferation and Cytotoxicity Assays. *J. Immunol. Methods* **1983**, *65*, 55–63.
- (44) Srivastava, A.; Ghorai, S.; Bhattacharjya, A.; Bhattacharya, S. A Tetrameric Sugar-Based Azobenzene That Gels Water at Various pH Values and in the Presence of Salts. *J. Org. Chem.* **2005**, *70*, 6574–6582.
- (45) Cai, X.; Wu, Y.; Wang, L.; Yan, N.; Liu, J.; Fang, X.; Fang, Y. Mechano-Responsive Calix[4]Arene-Based Molecular Gels: Agitation Induced Gelation and Hardening. *Soft Matter* **2013**, *9*, 5807–5814.
- (46) Ye, F.; Chen, S.; Tang, G. D.; Wang, X. Sonication Induced Morphological Transformation between 3D Gel Network and Globular Structure in a Two-Component Gelation System. *Colloids Surf., A* **2014**, *452*, 165–172.

(47) Zhou, Y.; Xu, M.; Yi, T.; Xiao, S.; Zhou, Z.; Li, F.; Huang, C. Morphology-Tunable and Photoresponsive Properties in a Self-Assembled Two-Component Gel System. *Langmuir* **2007**, *23*, 202–208.

(48) Nanda, J.; Biswas, A.; Banerjee, A. Single Amino Acid Based Thixotropic Hydrogel Formation and PH-Dependent Morphological Change of Gel Nanofibers. *Soft Matter* **2013**, *9*, 4198–4208.

(49) Haldar, D.; Drew, M. G. B.; Banerjee, A. α -Aminoisobutyric Acid Modified Protected Analogues of β -Amyloid Residue 17–20: A Change from Sheet to Helix. *Tetrahedron* **2006**, *62*, 6370–6378.

(50) Liu, Y.; Wang, T.; Liu, M. Supramolecular Polymer Hydrogels from Bolaamphiphilic L -Histidine and Benzene Dicarboxylic Acids: Thixotropy and Significant Enhancement of Eu III Fluorescence. *Chem. - Eur. J.* **2012**, *18*, 14650–14659.

(51) Castelletto, V.; Cheng, G.; Stain, C.; Connon, C. J.; Hamley, I. W. Self-Assembly of a Peptide Amphiphile Containing l -Carnosine and Its Mixtures with a Multilamellar Vesicle Forming Lipid. *Langmuir* **2012**, *28*, 11599–11608.

(52) Baral, A.; Roy, S.; Dehsorkhi, A.; Hamley, I. W.; Mohapatra, S.; Ghosh, S.; Banerjee, A. Assembly of an Injectable Noncytotoxic Peptide-Based Hydrogelator for Sustained Release of Drugs. *Langmuir* **2014**, *30*, 929–936.

(53) Pacios, L. F.; Gálvez, O.; Gómez, P. C. Variation of Geometries and Electron Properties along Proton Transfer in Strong Hydrogen-Bond Complexes. *J. Chem. Phys.* **2005**, *122*, 214307.

(54) Trachsel, M. A.; Ottiger, P.; Frey, H. M.; Pfaffen, C.; Bihlmeier, A.; Klopfer, W.; Leutwyler, S. Modeling the Histidine-Phenylalanine Interaction: The $\text{NH}\cdots\pi$ Hydrogen Bond of Imidazole-Benzene. *J. Phys. Chem. B* **2015**, *119*, 7778–7790.

(55) Guo, W. H.; Frey, M. T.; Burnham, N. A.; Wang, Y. L. Substrate Rigidity Regulates the Formation and Maintenance of Tissues. *Biophys. J.* **2006**, *90*, 2213–2220.

(56) Li, J.; Han, D.; Zhao, Y. P. Kinetic Behaviour of the Cells Touching Substrate: The Interfacial Stiffness Guides Cell Spreading. *Sci. Rep.* **2014**, *4*, 1–11.

(57) Vertelov, G.; Gutierrez, E.; Lee, S. A.; Ronan, E.; Groisman, A.; Tkachenko, E. Rigidity of Silicone Substrates Controls Cell Spreading and Stem Cell Differentiation. *Sci. Rep.* **2016**, *6*, 1–6.

(58) Solon, J.; Levental, I.; Sengupta, K.; Georges, P. C.; Janmey, P. A. Fibroblast Adaptation and Stiffness Matching to Soft Elastic Substrates. *Biophys. J.* **2007**, *93*, 4453–4461.

(59) Tee, S. Y.; Fu, J.; Chen, C. S.; Janmey, P. A. Cell Shape and Substrate Rigidity Both Regulate Cell Stiffness. *Biophys. J.* **2011**, *100*, 25–27.

(60) Scherzer, M. T.; Waigel, S.; Donniger, H.; Arumugam, V.; Zacharias, W.; Clark, G.; Siskind, L. J.; Soucy, P.; Beverly, L. Fibroblast-Derived Extracellular Matrices: An Alternative Cell Culture System That Increases Metastatic Cellular Properties. *PLoS One* **2015**, *10*, e0138065.

(61) Jansen, K. A.; Bacabac, R. G.; Piechocka, I. K.; Koenderink, G. H. Cells Actively Stiffen Fibrin Networks by Generating Contractile Stress. *Biophys. J.* **2013**, *105*, 2240–2251.